Published in final edited form as:
Sci Total Environ. 2024 May 20; 926: 171389. doi:10.1016/j.scitotenv.2024.171389.

Assessing the nucleic acid decay of human wastewater markers and enteric viruses in estuarine waters in Sydney, Australia

Warish Ahmed[a,*], **Asja Korajkic**[b], **Metasebia Gabrewold**[a], **Sudhi Payyappat**[c], **Michele Cassidy**[c], **Nathan Harrison**[c], **Colin Besley**[c]

[a]CSIRO Environment, Ecosciences Precinct, 41 Boggo Road, Dutton Park, QLD 4102, Australia

[b]United States Environmental Protection Agency, 26W Martin Luther King Jr. Drive, Cincinnati, OH 45268, United States

[c]Sydney Water, 1 Smith Street, Parramatta, NSW 2150, Australia

Abstract

This research investigated the in-situ decay rates of four human wastewater-associated markers (*Bacteroides* HF183 (HF183), *Lachnospiraceae* Lachno3 (Lachno3), cross-assembling phage (crAssphage), pepper mild mottle virus (PMMoV) and three enteric viruses (human adenovirus 40/41 (HAdV 40/41), enterovirus (EV) and human norovirus GII (HNoV GII) in two estuarine water environments (Davidson Park (DP) and Hen and Chicken Bay (HCB) in temperate Sydney, NSW, Australia, employing qPCR and RT-qPCR assays. The study also aimed to compare decay rates observed in mesocosms with previously published laboratory microcosms, providing insights into the persistence of markers and viruses in estuarine environments. Results indicated varying decay rates between DP and HCB mesocosms, with HF183 exhibiting relatively faster decay rates compared to other markers and enteric viruses in sunlight and dark mesocosms. In DP mesocosms, HF183 decayed the fastest, contrasting with PMMoV, which exhibited the slowest. Sunlight induced higher decay rates for all markers and viruses in DP mesocosms. In HCB sunlight mesocosms, HF183 nucleic acid decayed most rapidly compared to other markers and enteric viruses. In dark mesocosms, crAssphage showed the fastest decay, while PMMoV decayed at the slowest rate in both sunlight and dark mesocosms. Comparisons with laboratory microcosms revealed faster decay of markers and enteric viruses in laboratory

*Corresponding author. Warish.Ahmed@csiro.au (W. Ahmed).

Declaration of competing interest

The authors declare that they have no known competing financial interests or personal relationships that could have appeared to influence the work reported in this paper.

CRediT authorship contribution statement

Warish Ahmed: Writing – original draft, Methodology, Formal analysis, Conceptualization. **Asja Korajkic:** Writing – original draft, Formal analysis. **Metasebia Gabrewold:** Methodology. **Sudhi Payyappat:** Methodology. **Michele Cassidy:** Writing – original draft. **Nathan Harrison:** Writing – original draft. **Colin Besley:** Writing – original draft, Conceptualization.

Disclaimer

Information has been subjected to U.S. EPA peer and administrative review and has been approved for external publication. Any opinions expressed in this paper are those of the authors and do not necessarily reflect the official positions and policies of the U.S. EPA. Any mention of trade names or commercial products does not constitute endorsement or recommendation for use.

Appendix A. Supplementary data

Supplementary data to this article can be found online at https://doi.org/10.1016/j.scitotenv.2024.171389.

microcosms than the mesocosms, except for crAssphage and HAdV 40/41 in dark, and PMMoV in sunlight mesocosms. The study concludes that decay rates of markers and enteric viruses vary between estuarine mesocosms, emphasizing the impact of sunlight exposure, which was potentially influenced by the elevated turbidity at HCB estuarine waters. The generated decay rates contribute valuable insights for establishing site-specific risk-based thresholds of human wastewater-associated markers.

GRAPHICAL ABSTRACT

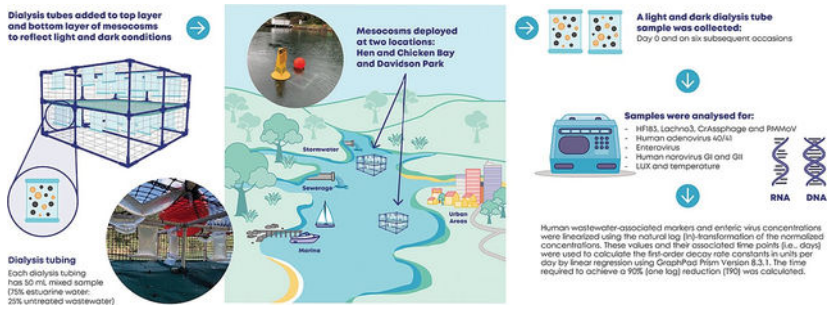

Keywords

Decay; Estuarine waters; Human health risks; Microbial source tracking; Wastewater pollution

1. Introduction

Pathogenic bacteria, viruses, and protozoa, pose a significant threat to both human and animal health by causing waterborne diseases (Collier et al., 2021; Ma et al., 2022). Pathogen entry into aquatic ecosystems stems from diverse sources, including untreated wastewater discharge, agricultural runoff, and stormwater discharge, as demonstrated by several studies (Huang et al., 2017; Steele et al., 2018; Fu et al., 2021). Monitoring of these pathogens in aquatic ecosystems is important, as it provides critical insights into water quality and associated health risks. However, the sheer diversity of potential pathogens presents an operational challenge for routine monitoring efforts. Furthermore, the detection and quantification of specific pathogens within water samples are hindered by their often-low concentrations, complex sample compositions, and the prerequisite for highly sensitive analytical techniques (Ramírez-Castillo et al., 2015).

Fecal Indicator Bacteria (FIB), including fecal coliforms, *Escherichia coli*, and enterococci, constitute a pivotal group of bacteria frequently employed as indicators of microbial water quality (OEH, 2011; Tiwari et al., 2021). These microorganisms are typically inhabitants of the intestines and fecal matter of warm-blooded animals including humans. Therefore, their presence in water signifies the potential for fecal contamination, thereby implying an associated risk of waterborne illnesses (Ahmed et al., 2013; Rochelle-Newall et al., 2015; Hughes et al., 2017). FIB are preferred in water quality monitoring programs for their cost-effectiveness and rapid detection capabilities, often yielding results within 24–48 h (Wade et al., 2010).

Nevertheless, it is essential to acknowledge the inherent limitations in relying solely on FIB as indicators of water quality. One limitation lies in their inability to provide information regarding the presence of pathogens capable of causing human illnesses (Abdelzaher et al., 2010; Wyn-Jones et al., 2011). The persistence and behaviour of FIB can differ significantly from that of pathogens (Abia et al., 2016; Greaves et al., 2020). Complicating matters further, FIB, including *E. coli*, can originate from sources other than fecal matter, such as soil and vegetation (Desmarais et al., 2002; Anderson et al., 2005; Ishii et al., 2006; Byappanahalli et al., 2012). Furthermore, it is critical to recognize that monitoring FIB alone does not provide insights into the sources of contamination (Harwood et al., 2014; Demeter et al., 2023).

Microbial source tracking (MST) is a valuable technique employed for the discernment and quantification of fecal pollution origins within aquatic systems (Scott et al., 2002). MST includes many techniques but mainly leverages host-specific genetic markers to ascertain the presence of contaminants from distinct sources, such as human, livestock, or wildlife origins (Ahmed et al., 2019; Linke et al., 2021). This information plays a pivotal role in pinpointing and mitigating pollution sources, thus safeguarding public health. MST has proven effective in diverse contexts, including coastal watersheds, recreational waters, and potable water reservoirs (Araújo et al., 2014; Ahmed et al., 2013; Ahmed et al., 2018).

In a recent study, human wastewater-associated markers and enteric viruses were detected across ten estuary locations in Sydney, NSW subjected to wet weather overflows (WWOs) (Ahmed et al., 2023a). Wet weather overflows discharge diluted sewage into receiving waters. However, human health risk associated with WWOs in complex estuarine waters is not well understood. The potential risk to human health in aquatic environments hinges on the degradation of human wastewater, fecal matter, and the pathogens they carry once introduced into water bodies (Nelson et al., 2018; Korajkic et al., 2019; Tiwari et al., 2023). A comprehension of the decay kinetics associated with human wastewater-associated markers, particularly of enteric viruses, in estuarine waters holds the potential to enhance health risk assessments and inform investments aimed at mitigating WWOs from sanitary sewage systems.

In a recent study, the degradation rates of wastewater indicators and enteric viruses were examined in laboratory-controlled microcosms replicating Sydney's temperate estuarine conditions (Ahmed et al., 2023b). Using quantitative and reverse-transcription quantitative polymerase chain reaction (qPCR/RT-qPCR), we found significant reductions in key human wastewater-associated markers such as *Bacteroides* HF183 (HF183), *Lachnospiraceae* Lachno3 (Lachno3), cross assembling phage (crAssphage), pepper mild mottle virus (PMMoV), human adenovirus (HAdV 40/41), and enterovirus (EV) over 42 days under artificial sunlight, dark and two different temperatures. The decay patterns varied depending on experimental conditions, with average T_{90} values ranging from days to months.

That recent study was conducted in a controlled laboratory setting, allowing precise experimentation but cannot fully replicate the complexity and variability of real-world estuarine ecosystems. For example, predation and competition, sunlight and temperatures may differ significantly from what occurs in the environmental waters. Therefore, the main

objective of this research study is to determine the in-situ decay rates of four human wastewater-associated markers (HF183, Lachno3, crAssphage and PMMoV) and three enteric viruses (HAdV 40/41, EV, and HNoV GII) in estuarine water environments in temperate Sydney, NSW, Australia using qPCR and RT-qPCR assays. A secondary objective was to compare the decay rates of these targets obtained for in-situ (mesocosms) decay to our previously published laboratory microcosms (Ahmed et al., 2023b) decay rates to understand how long these markers and viruses can persist in different settings, which is critical for public health and environmental management.

2. Materials and methods

2.1. Mesocosms set up and treatments

In-situ mesocosm decay experiments were conducted from 08/03/2021 to 15/04/2021. To carry out the decay experiments, grab estuarine water samples of 50 L were collected from Port Hacking at GPS coordinates: −34.08666; 151.09547, with a depth range of 0.5 to 1.5 m on 21/02/2021. Salinity, pH, dissolved oxygen, turbidity, and temperature were measured for estuarine water sample using a YSI EXO 2 sonde multiparameter meter (YSI Inc., Yellow Springs, OH, USA). The measurement of total organic carbon in estuarine water was conducted in the laboratory according to method APHA 5310B. In preparation for the mesocosm experiments, several 5-L grab samples of untreated municipal wastewater were obtained from the primary influent of two wastewater treatment plants (WWTPs) situated in Sydney, NSW, Australia. Bondi WWTP is located in North Bondi at coordinates −33.885397, 151.283728. This facility plays a crucial role in treating wastewater from approximately 500,000 residents living in the regions spanning from Bondi to Rozelle, which includes the central business district of Sydney. Conversely, the Cronulla WWTP, situated at coordinates −34.030902, 151.163707, is responsible for treating wastewater from an estimated 266,000 individuals. Collected estuarine water and untreated human wastewater were stored at 4 °C until the commencement of the study. A previous study demonstrated that the concentrations of human wastewater-associated markers were quite stable over the course of 12-month study with little variations observed within and between these two WWTPs (Ahmed et al., 2022).

Mesocosm experiments were conducted to assess the decay rates of markers associated with human wastewater and enteric viruses representing two different estuarine settings under ambient conditions. Davidson Park (DP) is about 10 km north of the Sydney central business district (CBD) in the channel of the upper Middle Harbour arm, 12 km to the mouth of Sydney Harbour. Hen and Chicken Bay (HCB) is a shallow embayment of the Parramatta River at the upper western arm of Sydney Harbour, approximately 10 km west of the Sydney CBD, and 17 km from the Sydney Harbour estuary mouth. Land cover in the DP urban catchment has native forest to the shoreline and more distant housing. In contrast to the DP catchment, land cover in the urban catchment of HCB is heavily urbanised, with a history of industrial and urban pollution impacts (Montoya, 2015).

To facilitate these experiments, two submersible mesocosm devices were constructed, following the design described by Korajkic et al. in 2014. These devices consisted of a polyvinyl chloride (PVC) pipe frame, with a diameter ranging from 3/4 to 1 in., enclosed

with plastic mesh wire. This setup was designed to protect the 50 mL dialysis tubes, which had a molecular weight cut-off (MWCO) of 6–8 kDa (Spectra/Por, Spectrum Laboratories, Inc., CA, USA), housed within them from potential damage caused by floating debris. The small pore size of the dialysis tubes prevents nutrients and microorganisms larger than 6–8 kDa from diffusing across the membrane. Each dialysis tube was filled with 75:25 % (*v*/v) of estuarine water: untreated sewage so that enteric viruses whose concentration are low, can be measured. Dialysis tubes were sealed with a reusable universal closure (Spectra/Por, Spectrum Laboratories, Inc.). One of the study goals was to examine the impact of sunlight exposure on the decay of human wastewater-associated markers and enteric viruses. Consequently, we divided each device into two sections: the lower half was covered with a black plastic sheet to create a dark treatment environment while the upper half remained uncovered to receive sunlight exposure (as depicted in graphical abstract). During deployment, the dialysis bags for the sunlight treatment were submerged approximately 0.5 m below the water's surface, while the dark treatment bags were submerged approximately 1.5 m below the surface. We assessed the potential attenuation of sunlight by the dialysis bags by measuring UV light intensity using a radiometer, both with and without the dialysis bag cover. The variance in UV readings was minimal, approximately around 8 %.

2.2. Sample processing and nucleic acid extraction

Dialysis tubes were collected on days 0, 3, 10, 13, 17, 24 and 38 (for DP mesocosms) and 0, 3, 10, 13, 17, 24 and 38 (for HCB mesocosms). Each dialysis tube was mixed by carefully inverting 8–10-times. A 50 mL water sample from each dialysis tube was removed and concentrated using an adsorption-extraction (AE) method (Ahmed et al., 2023b). Prior to filtration, the pH of the sample was adjusted to 3.5 by adding 2.0 N HCl (Ahmed et al., 2023b). Each sample was filtered through HA electronegative membranes with a 0.45 μm pore size (47 mm diameter) (Merck Millipore, Tokyo, Japan). Following filtration, the membrane was immediately removed, rolled, and inserted into a 5-mL-bead-beating tube (Qiagen, Hilden, Germany) for nucleic acid extraction. Nucleic acid was extracted directly from the HA membranes using the RNeasy PowerWater Kit (Cat. No. 14700–50-NF) (Qiagen, Valencia, CA). Prior to homogenization, lysis buffer was added into each bead-beating tube. The bead-beating tubes were then homogenized using a Precellys 24 tissue homogenizer (Bertin Technologies, Montigny-le-Bretonneux, FR) set for 3 × 15 s at 10,000 rpm at a 10 s interval. After homogenization, the tubes were centrifuged at 4000 *g* for 5 min to pellet the filter debris and beads. Sample lysate supernatant ranging from 600 to 800 μL in volume was then used to extract nucleic acid following the manufacturer's specified protocol. DNase treatment step was omitted from the extraction protocol to obtain both DNA and RNA from each sample. Nucleic acid purity was verified by measuring $A_{260/280}$ ratio using a DeNovix Spectrophotometer & Fluorometer (Wilmington, DE, USA).

2.3. PCR inhibition monitoring

An experiment was conducted to determine the presence of PCR inhibitors in nucleic acid extracted from water samples using a Sketa22 real-time PCR assay (Haugland et al., 2005; Ahmed et al., 2023b). Water samples with a 2-Cq (quantification cycle) delay were considered to have PCR inhibitors (Staley et al., 2012).

2.4. qPCR and RT-qPCR assays

Previously published qPCR and RT-qPCR assays were used for the analysis of HF183 (Green et al., 2014), Lachno3 (Feng et al., 2018), crAssphage (Stachler et al., 2017), PMMoV (Rosario et al., 2009; Haramoto et al., 2013), HAdV 40/41 (Ko et al., 2005), EV (Cashdollar et al., 2013) and human norovirus GI and GII (HNoV GI and GII) (Jothikumar et al., 2005). The primers and probes for these qPCR and RT-qPCR assays are shown in Supplementary Table ST1 along with qPCR cycling parameters. For all qPCR and RT-qPCR assays, synthetic DNA (4 μg) in plasmid cloning vectors or gBlocks gene fragments were purchased from Integrated DNA Technologies (Coralville, IA, USA).

qPCR and RT-qPCR standards were prepared from the synthetic DNA, ranging from 10^6 to 1 gene copy (GC)/μL of DNA. All qPCR amplifications were performed in 20 μL reaction mixtures using 10 μL SsoAdvanced Universal Probes Supermix (Bio-Rad Laboratories, Richmond, CA) or 100–1000 nM forward primer, 100–1000 nM of reverse primer, 80–400 nM probe and 3 μL of template nucleic acid. The qPCR assays were performed using a Bio-Rad CFX96 thermal cycler. All qPCR reactions were performed in triplicate. For each qPCR run, a series of standard (i.e., also served as PCR positive controls) and PCR negative controls ($n = 3$) were included.

2.5. Quality control and data analysis

A reagent and extraction blank were included for each batch of nucleic acid extraction to ensure no carryover contamination occurred during extraction. No carryover contamination was observed in reagent blank samples. To minimize qPCR contamination, nucleic acid extraction and qPCR setup were performed in separate laboratories. qPCR and RT-qPCR standards were analyzed to determine the amplification efficiencies (E) and the correlation coefficient (R^2). Plasmid controls were diluted (3×10^2 to 0.3 GC/reaction) and analyzed using qPCR and RT-qPCR. At each dilution, 12 replicates were analyzed. The 95 % assay limit of detection (ALOD) was defined by fitting an exponential survival model to the proportion of PCR replicates positive at each step along the gradient (Verbyla et al., 2016).

2.6. Data analysis

To facilitate comparisons with other studies, human wastewater-associated markers and enteric viruses' nucleic acid concentrations greater than the qPCR/RT-qPCR ALOD for each treatment were used to calculate the decay rate. Observed nucleic acid concentrations were linearized using the natural log (ln)-transformation of the normalized concentrations as shown in Eq. (1) (Chick, 1908). These values and their associated time points (i.e., days) were used to calculate the first-order decay rate constants in units per day by linear regression using GraphPad Prism Version 8.3.1 (GraphPad Software, La Jolla, CA, USA). The runs test was used to evaluate the appropriateness of the linear model, and fit was assessed by r^2 and root mean square error (RMSE). r^2 assesses the proportion of the variance explained by the independent variable given the selected model, while the RMSE assesses fit by measuring the distance of the observed measures from the fitted line.

$$\mathrm{Ln}(C_t/C_0) = -k^* \mathrm{T} \quad (1)$$

The first-order decay rate constant and the associated 95 % confidence interval were estimated by linear regression, where C_t and C_0 are the concentrations of GC in the mesocosms at time t and time 0, respectively, and k is the decay rate constant. The time required to achieve a 90 % (one log) reduction (T_{90}) was calculated using Eq. (2).

$$T_{90} = -\mathrm{Ln}(0.1)/k \quad (2)$$

After mean k values were estimated for each treatment, the values were $\log_{10}$–transformed and linear regression was used to characterize the relationship between treatments and first-order decay rate constant. We also calculated $\log_{10}$ reduction rates for human wastewater-associated markers and enteric viruses. The $\log_{10}$ reduction was calculated by subtracting the respective day zero concentrations from day 13 for DP and HCB *meso*cosms, and day 14 for laboratory microcosms (Ahmed et al., 2023b). These days were chosen because that was the last sampling point when all the targets were detected above their respective qPCR/RT-qPCR ALOD. Additionally, laboratory microcosm was not sampled on day 13.

2.7. Statistical analysis

GraphPad Prism was used to perform two-way ANOVA with Tukey's multiple comparison tests to evaluate the effect of each treatment on the $\log_{10}$ reduction rates of human-wastewater associated markers and enteric viruses (Tables ST5–ST9). The same software was used to perform the paired *t*-tests (comparison between DP and HCB mesocosms) and unpaired t-tests (comparison between DP mesocosms and laboratory microcosms and comparison between HCB mesocosms and laboratory microcosm) to evaluate the $\log_{10}$ reduction rates of each target between different meso/microcosms (Table ST9). All tests were considered significant if $\alpha = 0.05$.

3. Results

3.1. Physico-chemical parameters of mesocosm samples

During the sampling period, various physico-chemical parameters were measured in dialysis tubes water sample deployed at two estuarine sites, namely DP and HCB sunlight and dark mesocosms. The salinity at DP exhibited a range of 28.1 ± 6.86 to 32.4 ± 1.86 ppt in sunlight and dark mesocosms, respectively, while HCB showed values ranging from 28.9 ± 8.92 to 30.0 ± 5.78 ppt (Supplementary Table ST2). The pH levels at DP were 7.57 ± 0.18 (sunlight) and 7.62 ± 0.13 (dark), whereas HCB recorded values of 7.84 ± 0.22 and 7.81 ± 0.13 in sunlight and dark mesocosms, respectively. Dissolved oxygen concentrations at DP ranged from 4.76 ± 1.21 to 3.97 ± 1.04 mg/L in sunlight and dark mesocosms, while HCB displayed values of 7.18 ± 2.06 and 6.37 ± 0.98, respectively. Turbidity measurements at DP were 2.46 ± 2.49 (sunlight) and 2.20 ± 0.75 (dark), while at HCB, they were 5.47 ± 3.10

and 6.44 ± 3.10 in sunlight and dark mesocosms, respectively. The temperature at both sites remained relatively stable, with DP recording 23.5 ± 1.17 (sunlight) and 23.6 ± 0.98 (dark), and HCB showing values of 23.5 ± 1.88 and 23.2 ± 1.75 in sunlight and dark mesocosms, respectively. These data provide insights into the dynamic environmental conditions within the two estuarine ecosystems during the specified sampling period.

Throughout the study period, the temperatures of the water within the mesocosms remained relatively constant. In the DP mesocosm, the average temperatures were documented at 24.6 °C under sunlight and 24.8 °C in the dark. Similarly, in the HCB mesocosm, temperatures were comparable, registering at 24.5 °C under sunlight and 22.2 °C in the dark, as recorded by HOBO data loggers (refer to Supplementary Table ST3). The amount of sunlight received by the DP and HCB mesocosms ranged from 0 to 39,761 and 0 to 64,737 lm/ft^2, respectively. In dark mesocosms, the DP and HCB mesocosms received between 0 and 626, and 0 to 1497 lm/ft^2, respectively.

3.2. qPCR/RT-qPCR performance characteristics

Standard curves exhibited a linear quantification range spanning from 3×10^6 to 3 GC/reaction. Supplementary Table ST4 presents performance characteristics for various assays based on efficiency (E), linearity (R^2), slope, and y-intercept. HF183 demonstrates an efficiency of 99.2 %, a high linearity of 0.99, with a slope of −3.342 and a y-intercept of −39.21. Similarly, crAssphage exhibited 101 % efficiency, 0.99 linearity, a slope of −3.301, and a y-intercept of −38.27. Lachno3, PMMoV, HAdV 40/41, EV, HNoV GI, and HNoV GII also show varying levels of efficiency and linearity with corresponding slope and y-intercept values that fell within the optimal range recommended by the MIQE guidelines (Bustin et al., 2009). The analytical limit of detection (ALOD) values for qPCR and RT-qPCR ranged from 6.02 to 21.7 GC/reaction (Ahmed et al., 2023b). There were no indications of carryover contamination observed in either the method or reagent blank samples. Nucleic acid contamination was diligently monitored throughout the study using no template controls, and there was no detected inhibition of PCR in the nucleic acid extracted from mesocosm samples.

3.3. Decay rates of wastewater-associated markers and enteric viruses in DP mesocosms

The decay rates (mean k values with 95 % CI) and mean T_{90} days with 95 % CI of human wastewater-associated markers and enteric viruses in DP mesocosms are shown in Table 1. Among the human-wastewater associated markers and enteric viruses, HF183 decayed the fastest, while the decay of PMMoV was the slowest in both sunlight and dark mesocosms. For HF183, the mean first-order decay rate constant (k) in sunlight were −0.414/day, resulting in a T_{90} of 5.56 days, while in the dark, the decay rate was −0.240/day with a T_{90} of 9.59 days. Under sunlight, PMMoV displayed a decay rate of −0.162/day corresponding to a T_{90} of 14.2 days. In the dark, the decay rate was lower at −0.087/day and the T_{90} was notably greater at 26.5 days compared to other markers at the same condition. The decay patterns revealed striking similarities between Lachno3 and crAssphage within the DP mesocosms under sunlight (Lachno3 showing a rate of −0.272 and crAssphage at −0.259). Overall, HF183 (k = −0.414), Lachno3 (k = −0.272) and crAssphage (k = −0.259) decayed slightly faster than HAdV 40/41 (k = −0.237) and HNoV GII (−0.181), while EV

($k = -0.268$) decayed slower than HF183 ($k = -0.414$) in sunlight mesocosms. However, in dark mesocosms, HF183 ($k = -0.240$), Lachno3 ($k = -0.182$), and crAssphage ($k = -0.233$) decayed faster than all three enteric viruses. Between the sunlight and dark mesocosms, sunlight induced greater decay rates of all human wastewater-associated markers and enteric viruses (Table 1).

3.4. Decay rates of wastewater-associated markers and enteric viruses in HCB mesocosms

Table 2 displays the mean k values and T_{90} days with 95 % CI of human wastewater-associated markers and enteric viruses in HCB mesocosms. HF183 nucleic acid degraded most quickly in sunlight mesocosms among human-wastewater markers and enteric viruses. In dark mesocosms, crAssphage exhibited the fastest decay, whereas PMMoV decayed at the slowest rate in both sunlight and dark mesocosms. The mean k in sunlight for HF183 was −0.328/day, leading to a T_{90} of 7.01 days, whereas crAssphage exhibited a decay rate of −0.200/day, resulting in a T_{90} of 11.5 days. In sunlight, PMMoV exhibited a decay rate of −0.064/day, resulting in a T_{90} of 36.0 days. Contrastingly, in dark mesocosms, the decay rate was −0.056/day, with the T_{90} extending to 41.1 days. The decay trends unveil remarkable parallels between HF183 and crAssphage in the HCB mesocosms, whether exposed to sunlight (HF183 demonstrating a rate of −0.328 and crAssphage at −0.289) or in the dark (HF183 at −0.195 and crAssphage at −0.200). Similar trends were also noted in dark mesocosms for both wastewater-associated markers and enteric viruses. In the interplay of sunlight and dark mesocosms, HF183, Lachno3, crAssphage, PMMoV, and HAdV 40/41 exhibited slightly higher decay rates under sunlight compared to dark mesocosms. Conversely, EV and HNoV GII displayed the opposite trend, with these two enteric viruses decaying slightly faster in dark mesocosms (Table 2).

3.5. Comparison of decay rates of wastewater-associated markers and enteric viruses between DP, HCB mesocosms and laboratory microcosms

In a recent study, we assessed the decay rates of markers and enteric viruses associated with human wastewater in laboratory microcosms designed to replicate estuarine water conditions in temperate Sydney, NSW, Australia using qPCR and RT-qPCR assays (Ahmed et al., 2023b). This basis allowed comparison to the decay rates observed in the current study with those in that previous study to gain insights into the persistence of these markers between mesocosms and microcosms. Notably, most human wastewater-associated markers and enteric viruses exhibited faster decay in DP than in HCB mesocosms, except for crassphage in sunlight ($k = -0.289$ in HCB and $k = -0.259$ in DP), EV ($k = -0.113$ in HCB and $k = -0.097$ in DP) and HNoV GII ($k = -0.147$ in HCB and $k = -0.115$ in DP).

Comparisons revealed that the decay rates of HF183 (both in sunlight and dark mesocosms), Lachno3, crAssphage, and HAdV 40/41 (in sunlight), as well as EV (in both sunlight and dark mesocosms), were marginally faster in laboratory microcosms than the DP and HCB mesocosms. Lachno3, crAssphage, PMMoV, and HAdV 40/41 in dark microcosms exhibited a slower decay rate compared to DP and HCB mesocosms. The sunlight treatment consistently led to accelerated decay rates and lower T_{90} values for markers and enteric viruses in both DP and HCB mesocosms and in laboratory microcosms. In several instances,

the decay rates of markers and enteric viruses closely resembled each other between mesocosms (this study) and laboratory microcosms (Table 3) (Ahmed et al., 2023b).

3.6. The effect of sunlight and dark treatments on log_{10} reduction values of markers and enteric viruses

For both mesocosms, exposure to sunlight and the type of markers and enteric viruses were significant contributors to decay $p < 0.0001$ (Table ST5). The percentage of contribution to the variability in the dataset was higher for the type of marker/virus (39–68 %) compared to sunlight exposure (6–11 %) (Table ST5). Of note, the interaction of variables was also significant factor (Table ST5) suggesting that the effect of sunlight exposure is dependent on the marker/virus.

For the DP mesocosm, exposure to sunlight significantly accelerated the decay of HF183, Lachno3 and EV ($p \leq 0.0152$), but it's effect on the remainder of the markers/viruses was unremarkable (Table ST6). In the DP mesocosm under sunlight exposure, HF183 decayed faster than any other marker/virus ($p < 0.0001$), and Lachno3 decayed faster than most of the viruses studied ($p \leq 0.0039$) (Table ST7). CrAssphage decay was generally like that of other markers/viruses, while PMMoV tended to be the most persistent compared to other markers/viruses ($p < 0.0001$) (Table ST7). Enteric virus decay (i.e., EV, HAdV 40/41, and HNoV GII) was faster compared to PMMoV ($p < 0.0001$) but there was no difference in comparisons with the crAssphage (Table ST7). In the dark mesocosms, the patterns of decay were similar. HF183 and Lachno3 generally decayed faster than any of the enteric viruses ($p \leq 0.0074$), PMMoV was the most resilient, and the decay of enteric viruses was generally faster than PMMoV and crAssphage ($p < 0.001$) (Table ST7).

In the HCB mesocosms, the effect of sunlight exposure was not as pronounced as it affected the decay of HF183 only ($p < 0.0001$) (Table ST8). Aside from that, the general patterns of decay were similar to what was observed for the DP mesocosms. In sunlight mesocosms, the decay rates of HF183 and Lachno3 was generally faster compared to other markers/viruses ($p \leq 0.0039$), PMMoV was the most persistent, and enteric viruses tended to decay faster than either PMMoV or crAspphage ($p \leq 0.0188$) (Table ST8). Interestingly, in the dark mesocosms, HF183 decayed slower than any other marker/virus, while the crAssphage decayed the most ($p < 0.0001$) (Table ST8). Lachno3 continued to decay generally faster than most viruses ($p \leq 0.0004$). The PMMoV remained the most resilient marker, and enteric virus decay was faster compared to PMMoV ($p \leq 0.0187$), but not any other markers/viruses (Table ST8).

Comparison of decay of markers/enteric viruses between DP and HCB mesocosms, indicated that crAssphage, HAdV 40/41 and EV decayed faster in the sunlight mesocosms ($p \leq 0.0172$), and HF183, PMMoV and HAdV 40/41 decayed faster in dark mesocosms ($p \leq 0.0082$) in DP vs. HCB (Table ST9). Lachno3 is the only marker that decayed faster in HCB vs. DP ($p = 0.0269$), but there were no other statistically significant results (Table ST9). Comparisons between DP mesocosms and laboratory microcosms, as well between HCB mesocosms and laboratory microcosms were remarkably similar. For the DP comparison, under both sunlight and dark conditions, all markers/viruses except PMMoV decayed faster in laboratory microcosms compared to DP mesocosms ($p \leq 0.0046$) (Table

ST9). In the comparisons between HCB mesocosms and laboratory microcosms, there was no statistically significant difference for HAdV 40/41 (sunlight and dark) and PMMoV (sunlight only) (Table ST9). In sunlight mesocosms, HF183, Lachno3, crAssphage and EV decayed faster in the laboratory microcosms ($p < 0.0001$) compared to the HCB mesocosms. In the dark mesocosms, HF183 and Lachno3 decayed faster in the laboratory microcosms ($p < 0.0001$), but opposite was observed for crAssphage and PMMoV ($p \leq 0.0275$) (Table ST9).

4. Discussion

In our recent study, we reported the occurrence of HAdV 40/41, EV, alongside four specific human wastewater-associated markers: crAssphage, HF183, Lachno3, and PMMoV at ten estuary locations linked to WWOs (Ahmed et al., 2023a). In a subsequent study, we documented a decrease in these markers and enteric viruses within two estuarine waters over seven- and 12-days post WWOs (Ahmed et al., 2023c). Nevertheless, determining whether the observed reduction resulted from actual decay, tidal influences, or sedimentation presented a challenge. Therefore, we conducted a controlled laboratory microcosm study to determine the decay rates of these markers and enteric viruses under artificial sunlight, dark and two different temperatures mimicking real-world estuarine conditions (Ahmed et al., 2023b).

The decay trends exhibited variations based on experimental circumstances, resulting in average T_{90} durations spanning from days to months. Although these investigations occurred in meticulously controlled laboratory environments, facilitating precise experimentation, they could not fully emulate the intricacies and fluctuations found in real-world estuarine ecosystems. Consequently, the current study focused on determining in-situ decay rates of markers associated with human wastewater and enteric viruses in estuarine water environments in temperate Sydney, NSW, Australia. The overarching goals of these studies were to offer a nuanced comprehension of how the nucleic acid from these microbial targets reacts to environmental conditions. This approach sheds light on their decay dynamics and fate in the environment.

For the mesocosm study, instead of using sealed microcosms such as glass bottles or vials, we opted for the use of dialysis tubes (Korajkic et al., 2014; Mattioli et al., 2017). These tubes allowed the passage of solutes, replicating conditions relevant to estuarine waters, while preventing the entry or exit of microorganisms or particles >6–8 kDa. A meta-analysis of decay studies on MST markers and fecal indicator bacteria suggested that sealed microcosms may have limited value in understanding the decay of these targets in the environment (Brooks and Field, 2016). Notably, dialysis tubes offer the advantage of allowing approximately 80 % transmission of sunlight within the 280–700 nm wavelength range (Maraccini et al., 2016). Specifically, the dialysis tubing used in our study was found to be permissible to the sunlight as it blocked <10 % of UV irradiation (Korajkic et al., 2014). A drawback associated with dialysis bags is the risk of leakage in fast-flowing waters and susceptibility to biofouling. We observed both occurrences during the decay study, prompting us to suggest the deployment of extra dialysis bags as a precaution against potential leaks.

To simulate real-life scenarios of sewage pollution, instead of using laboratory-cultivated strains, untreated sewage was used as an inoculum. The use of sewage as an inoculum provides the benefit of high concentrations of most microbial targets, facilitating their quantification over time. Among the markers associated with human wastewater and enteric viruses, only NoV GI was not detectable in human wastewater samples. Consequently, the decay rates of NoV GI could not be determined in this study. However, we were able to measure the decay rates of NoV GII, and it is likely that the decay rate of NoV GI will be similar to NoV GII. Mattioli et al. (2017) similarly sought to ascertain the decay of NoV in marine waters by introducing 50 mL of sewage into 1 L of water; however, the concentration of NoV in the inoculum was low. In this study, we added 25 mL of sewage into 75 mL of estuarine water which allowed us the detection of NoV GII. The current study took place during the swimming season in NSW, with two different swimming sites (DP and HCB) selected to explore environmental variability and its impact on the decay of the selected markers/viruses.

The site selection and the environmental conditions unique to DP and HCB affected the decay of HF183, Lachno3, PMMoV, HAdV 40/41 and crAssphage with most of them decaying faster at the DP site. Notably, the decay of enteric viruses was similar between the sites. While sunlight (Table ST1), salinity and pH were similar between the sites, the HCB had somewhat higher turbidity measurements (Table ST2). The elevated turbidity at HCB site likely slowed down the decay as it affected exposure of dialysis bags to sunlight effectively causing molecular shading. Similar findings were reported for the decay of enterococci in marine and estuarine waters (Kay et al., 2005), while others showed negative correlation between elevated turbidity and ability of the sunlight to penetrate lake water as well as rainwater (Amin and Han, 2009; Whitman et al., 2004). It is also possible that higher particulate matter at HCB allowed for binding of bacteria and viruses (and their nucleic acids) allowing for prolonged persistence. Comparison of decay between mesocosms (both DP and HCB) to that in laboratory microcosms, indicated generally faster decay of all analytes in the laboratory microcosms which is not surprising given the artificial conditions of closed microcosm system. However, there were a few notable exceptions where crAssphage, PMMoV and HAdV 40/41 decayed faster in the mesocosms compared to microcosms. Likely reason for this observation is that completely dark conditions cannot be created when experiments are conducted in situ. Indeed, our sunlight measurements (Table ST4) indicated that some sunlight was still reaching the dark treatments for both mesocosms. Studies conducted under similar conditions have shown comparable findings (Korajkic et al., 2023; McMinn et al., 2020).

The influence of ambient sunlight on microbial decay is arguably one of the most extensively studied environmental parameters. In our study, decay was generally faster in sunlight, and this was especially evident for the DP mesocosms. In these mesocosms, HF183, Lachno3 and EV decayed faster in sunlight but not PMMoV, HAdV 40/41 or HNoV GII. The resilience of PMMoV and HAdV 40/41 to degradation by sunlight has been described before (Bae and Wuertz, 2012) and similar has been suggested for HNoV through a recent systematic literature review (Boehm et al., 2019). In the HCB mesocosms exposed to sunlight accelerated the decay of only HF183 and this is likely a consequence of turbidity differences discussed earlier. While sunlight has been generally shown to accelerate

the decay of bacteria and viruses (and their nucleic acids), the effects are dependent on many different factors including turbidity, dissolved oxygen, sunlight intensity, time of the year and geographic region making it difficult to extrapolate our findings to other studies.

In this study, PMMoV persisted longer than any other analyte in both mesocosms. This is similar to the observation we made in our earlier study (Ahmed et al., 2023b), and consistent with its persistence through wastewater treatment train (Rosario et al., 2009; Hamza et al., 2011; Kitajima et al., 2014; Symonds et al., 2014). Combination of extended persistence and frequent detection in wastewater and surface waters (Kitajima et al., 2018), make PMMoV a conservative indicator of human fecal pollution in the environment. On the other hand, bacterial markers (HF183 and Lachno3), generally decayed faster than viral markers and enteric viruses. This observation is consistent with our earlier work, and that of others (Ahmed et al., 2023b; Mattioli et al., 2017). This is not surprising considering the inherent differences between the taxonomic groups. Furthermore, the accelerated decay of HF183 and Lachno3 suggests that when detected in surface waters, both markers are likely indicative of recent human fecal pollution but may not be indicative of viral pathogen presence. Interestingly, the decay of crAssphage was typically similar to that of enteric viruses suggesting that it may be a better surrogate for viral pathogens in temperate estuarine environments. Finally, all three enteric viral pathogens decayed similarly irrespective of the study site and exposure to sunlight. This finding is important as it suggests that a singular viral indicator, such as crAssphage, has the potential to be adequate surrogate for multiple viral pathogens.

5. Conclusions

- The decay rates of human wastewater-associated markers and enteric viruses varied significantly between DP and HCB mesocosms. HF183 consistently exhibited faster decay in both sunlight and dark mesocosms, whereas crAssphage decayed faster in HCB mesocosms under sunlight but displayed similar rates in the dark compared to DP mesocosms.
- Sunlight exposure had a notable impact on the decay rates of markers/viruses in both DP and HCB mesocosms. Generally, human markers and enteric viruses decayed faster under sunlight, with HF183, Lachno3, and EV showing particularly accelerated decay in DP mesocosms.
- Distinct patterns in the decay rates were observed among markers/viruses. HF183 consistently decayed faster than other markers/viruses, especially under sunlight conditions, while PMMoV tended to be the most persistent. Enteric viruses, including EV, HAdV 40/41, and HNoV GII, displayed faster decay rates than PMMoV and crAssphage, both in sunlight and dark mesocosms.
- When compared to laboratory microcosms replicating estuarine water conditions, most markers and viruses decayed faster in DP and HCB mesocosms. However, some exceptions, such as crAssphage in sunlight and EV, displayed faster decay in laboratory microcosms.

- Decay rates of wastewater-associated markers and enteric viruses generated in this study could inform site-specific risk-based thresholds of human wastewater-associated markers.

Supplementary Material

Refer to Web version on PubMed Central for supplementary material.

Acknowledgements

We thank Sydney Water for financial assistance and for support in collection of samples and laboratory work. We also thank Sydney Water staff member Kaye Power for providing valuable feedback on the manuscript.

Data availability

Data will be made available on request.

References

Abdelzaher AM, Wright ME, Ortega C, Solo-Gabriele HM, Miller G, Elmir S, Newman X, Shih P, Bonilla JA, Bonilla TD, Palmer CJ, Scott T, Lukasik J, Harwood VJ, McQuaig S, Sinigalliano C, Gidley M, Plano LRW, Zhu X, Wang JD, Fleming LE, 2010. Presence of pathogens and indicator microbes at a non-point source subtropical recreational marine beach. Appl. Environ. Microbiol. 76, 724–732. [PubMed: 19966020]

Abia AL, Ubomba-Jaswa E, Momba MN, 2016. Competitive survival of *Escherichia coli*, V*ibrio cholerae*, *salmonella* t*yphimurium* and *Shigella dysenteriae* in riverbed sediments. Microb. Ecol. 72, 881–889. [PubMed: 27193001]

Ahmed W, Sritharan T, Palmer A, Sidhu JP, Toze S, 2013. Evaluation of bovine feces-associated microbial source tracking markers and their correlations with fecal indicators and zoonotic pathogens in a Brisbane, Australia, reservoir. Appl. Environ. Microbiol. 79, 2682–2691. [PubMed: 23417003]

Ahmed W, Hamilton KA, Lobos A, Hughes B, Staley C, Sadowsky MJ, Harwood VJ, 2018. Quantitative microbial risk assessment of microbial source tracking markers in recreational water contaminated with fresh untreated and secondary treated sewage. Environ. Int. 117, 243–249. [PubMed: 29772486]

Ahmed W, Bivins A, Payyappat S, Cassidy M, Harrison N, Besley C, 2022. Distribution of human fecal marker genes and their association with pathogenic viruses in untreated wastewater determined using quantitative PCR. Water Res. 226, 119093. [PubMed: 36252296]

Ahmed W, Gyawali P, Feng S, McLellan SL, 2019. Host specificity and sensitivity of established and novel sewage-associated marker genes in human and nonhuman fecal samples. Appl. Environ. Microbiol. 85 e00641–19. [PubMed: 31076423]

Ahmed W, Payyappat S, Cassidy M, Harrison N, Besley C, 2023a. Microbial source tracking of untreated human wastewater and animal scats in urbanized estuarine waters. Sci. Total Environ. 877, 162764. [PubMed: 36907409]

Ahmed W, Korajkic A, Smith WJ, Payyappat S, Cassidy M, Harrison N, Besley C, 2023b. Comparing the decay of human wastewater-associated marker genes and enteric viruses in laboratory microcosms simulating estuarine waters in a temperate climatic zone. Sci. Total Environ. 23, 167845.

Ahmed W, Payyappat S, Cassidy M, Harrison N, Besley C, 2023c. Reduction of human fecal markers and enteric viruses in Sydney estuarine waters receiving wet weather overflows. Sci. Total Environ. 896, 165008. [PubMed: 37348731]

Amin MT, Han M, 2009. Roof-harvested rainwater for potable purposes: application of solar disinfection (SODIS) and limitations. Water Sci. Technol. 60, 419–431. [PubMed: 19633384]

Anderson KL, Whitlock JE, Harwood VJ, 2005. Persistence and differential survival of fecal indicator bacteria in subtropical waters and sediments. Appl. Environ. Microbiol. 71, 3041–3048. [PubMed: 15933000]

Araújo S, Henriques IS, Leandro SM, Alves A, Pereira A, Correia A, 2014. Gulls identified as major source of fecal pollution in coastal waters: a microbial source tracking study. Sci. Total Environ. 470–471, 84–91.

Bae S, Wuertz S, 2012. Survival of host-associated bacteroidales cells and their relationship with *Enterococcus* spp., *Campylobacter jejuni*, *Salmonella* enterica serovar Typhimurium, and adenovirus in freshwater microcosms as measured by propidium monoazide-quantitative PCR. Appl. Environ. Microbiol. 78, 922–932. [PubMed: 22139002]

Boehm AB, Silverman AI, Schriewer A, Goodwin K, 2019. Systematic review and meta-analysis of decay rates of waterborne mammalian viruses and coliphages in surface waters. Water Res. 164, 114898. [PubMed: 31404902]

Brooks LE, Field KG, 2016. Bayesian meta-analysis to synthesize decay rate constant estimates for common fecal indicator bacteria. Water Res. 104, 262–271. [PubMed: 27543910]

Bustin SA, Benes V, Garson JA, Hellemans J, Huggett J, Kubista M, Mueller R, Nolan T, Pfaffl MW, Shipley GL, Vandesompele J, Wittwer CT, 2009. The MIQE guidelines: minimum information for publication of quantitative real-time PCR experiments. Clin. Chem. 55, 611–622. [PubMed: 19246619]

Byappanahalli MN, Roll BM, Fujioka RS, 2012. Evidence for occurrence, persistence, and growth potential of *Escherichia coli* and enterococci in Hawaii's soil environments. Microbes Environ. 27, 164–170. [PubMed: 22791049]

Cashdollar JL, Brinkman NE, Griffin SM, McMinn BR, Rhodes ER, Varughese EA, Grimm AC, Parshioniker SU, Wymer L, Fout GS, 2013. Development and evaluation of EPA method 1615 for detection of enterovirus and norovirus in water. Appl. Environ. Microbiol. 79, 215–223. [PubMed: 23087037]

Chick H, 1908. An investigation of the laws of disinfection. J. Hyg. (Lond). 8, 92–158. [PubMed: 20474353]

Collier SA, Deng L, Adam EA, Benedict KM, Beshearse EM, Blackstock AJ, Bruce BB, Derado G, Edens C, Fullerton KE, Gargano JW, Geissler AL, Hall AJ, Havelaar AH, Hill VR, Hoekstra RM, Reddy SC, Scallan E, Stokes EK, Yoder JS, Beach MJ, 2021. Estimate of burden and direct healthcare cost of infectious waterborne disease in the United States. Emerg. Infect. Dis. 27, 140–149. [PubMed: 33350905]

Demeter K, Linke R, Ballesté E, Reischer G, Mayer RE, Vierheilig J, Kolm C, Stevenson ME, Derx J, Kirschner AKT, Sommer R, Shanks OC, Blanch AR, Rose JB, Ahmed W, Farnleitner AH, 2023. Have genetic targets for faecal pollution diagnostics and source tracking revolutionized water quality analysis yet? FEMS Microbiol. Rev. 47, fuad028.

Desmarais TR, Solo-Gabriele HM, Palmer CJ, 2002. Influence of soil on fecal indicator organisms in a tidally influenced subtropical environment. Appl. Environ. Microbiol. 68, 1165–1172. [PubMed: 11872464]

Feng S, Bootsma M, McLellan SL, 2018. Novel human associated Lachnospiraceae genetic markers improve detection of fecal pollution sources in urban waters. Appl. Environ. Microbiol. 84, e00309–e00318. [PubMed: 29728386]

Fu S, Yang Q, Sheng Y, Wang Q, Wu J, Qiu Z, Lan R, Wang Y, Liu Y, 2021. Metagenomics combined with comprehensive validation as a public health risk assessment tool for urban and agricultural run-off. Water Res. 209, 117941. [PubMed: 34920315]

Greaves J, Stone D, Wu Z, Bibby K, 2020. Persistence of emerging viral fecal indicators in large-scale freshwater mesocosms. Water Res. X. 9, 100067.

Green HC, Haugland RA, Varma M, Millen HT, Borchardt MA, Field KG, Walters WA, Knight R, Sivaganesan M, Kelty CA, Shanks OC, 2014. Improved HF183 quantitative real-time PCR assay for characterization of human fecal pollution in ambient surface water samples. Appl. Environ. Microbiol. 80, 3086–3094. [PubMed: 24610857]

Hamza IA, Jurzik L, Überla K, Wilhelm M, 2011. Evaluation of pepper mild mottle virus, human picobirnavirus and torque Teno virus as indicators of fecal contamination in river water. Water Res. 45, 1358–1368. [PubMed: 21074236]

Haramoto E, Kitajima M, Kishida N, Konno Y, Katayama H, Asami M, Akiba M, 2013. Occurrence of pepper mild mottle virus in drinking water sources in Japan. Appl. Environ. Microbiol. 79, 7413–7418. [PubMed: 24056461]

Harwood VJ, Staley C, Badgley BD, Borges K, Korajkic A, 2014. Microbial source tracking markers for detection of fecal contamination in environmental waters: relationships between pathogens and human health outcomes. FEMS Microbiology Rev 38, 1–40.

Haugland RA, Siefring SC, Wymer LJ, Brenner KP, Dufour AP, 2005. Comparison of Enterococcus measurements in freshwater at two recreational beaches by quantitative polymerase chain reaction and membrane filter culture analysis. Water Res. 39, 559–568. [PubMed: 15707628]

Huang C, Hu Y, Wang L, Wang Y, Li N, Guo Y, Feng Y, Xiao L, 2017. Environmental transport of emerging human-pathogenic Cryptosporidium species and subtypes through combined sewer overflow and wastewater. Appl. Environ. Microbiol. 83 e00682–17. [PubMed: 28600310]

Hughes B, Beale DJ, Dennis PG, Cook S, Ahmed W, 2017. Cross-comparison of human wastewater-associated molecular markers in relation to fecal indicator bacteria and enteric viruses in recreational beach waters. Appl. Environ. Microbiol. 83 e00028–17. [PubMed: 28159789]

Ishii S, Ksoll WB, Hicks RE, Sadowsky MJ, 2006. Presence and growth of naturalized Escherichia coli in temperate soils from Lake Superior watersheds. Appl. Environ. Microbiol. 72, 612–621. [PubMed: 16391098]

Jothikumar N, Lowther JA, Henshilwood K, Lees DN, Hill VR, Vinjé J, 2005. Rapid and sensitive detection of noroviruses by using TaqMan-based one-step reverse transcription-PCR assays and application to naturally contaminated shellfish samples. Appl. Environ. Microbiol. 71, 1870–1875. [PubMed: 15812014]

Kay D, Stapleton CM, Wyer MD, McDonald AT, Crowther J, Paul N, Jones K, Francis C, Watkins J, Wilkinson J, Humphrey N, Lin B, Yang L, Falconer RA, Gardner S, 2005. Decay of intestinal enterococci concentrations in high-energy estuarine and coastal waters: towards real-time T90 values for modelling faecal indicators in recreational waters. Water Res. 39, 655–667. [PubMed: 15707639]

Kitajima M, Iker BC, Pepper IL, Gerba CP, 2014. Relative abundance and treatment reduction of viruses during wastewater treatment processes – identification of potential viral indicators. Sci. Total Environ. 488–489, 290–296.

Kitajima M, Sassi HP, Torrey JR, 2018. Pepper mild mottle virus as a water quality indicator. npj Clean Water 1, 19.

Ko G, Jothikumar N, Hill VR, Sobsey M, 2005. Rapid detection of infectious adenovirus by mRNA real-time RT-PCR. J. Virol. Methods 127, 148–153. [PubMed: 15967237]

Korajkic A, McMinn BR, Shanks OC, Sivaganesan M, Fout GS, Ashbolt NJ, 2014. Biotic interactions and sunlight affect persistence of fecal indicator bacteria and microbial source tracking genetic markers in the upper Mississippi river. Appl. Environ. Microbiol. 80, 3952–3961. [PubMed: 24747902]

Korajkic A, Wanjugi P, Brooks L, Cao Y, Harwood VJ, 2019. Persistence and decay of fecal microbiota in aquatic habitats. Microbiol. Mol. Biol. Rev. 83, e00005–e00019. [PubMed: 31578217]

Korajkic A, McMinn BR, Harwood VJ, 2023. The effect of protozoa indigenous to lakewater and wastewater on decay of fecal indicator bacteria and coliphage. Pathogens 12, 378. [PubMed: 36986300]

Linke RB, Kebede G, Mushi D, Lakew A, Hayes DS, Graf W, Farnleitner AH, 2021. Assessing the faecal source sensitivity and specificity of ruminant and human genetic microbial source tracking markers in the central Ethiopian highlands. Lett. Appl. Microbiol. 72, 458–466. [PubMed: 33300161]

Ma JY, Li MY, Qi ZZ, Fu M, Sun TF, Elsheikha HM, Cong W, 2022. Waterborne protozoan outbreaks: an update on the global, regional, and national prevalence from 2017 to 2020 and sources of contamination. Sci. Total Environ. 806, 150562. [PubMed: 34852432]

Maraccini PA, Mattioli MC, Sassoubre LM, Cao Y, Griffith JF, Ervin JS, Van De Werfhorst LC, Boehm AB, 2016. Solar inactivation of enterococci and Escherichia coli in natural waters: effects of water absorbance and depth. Environ. Sci. Technol. 50, 5068–5076. [PubMed: 27119980]

Mattioli MC, Sassoubre LM, Russell TL, Boehm AB, 2017. Decay of sewage-sourced microbial source tracking markers and fecal indicator bacteria in marine waters. Water Res. 108, 106–114. [PubMed: 27855952]

McMinn BR, Rhodes ER, Huff EM, Korajkic A, 2020. Decay of infectious adenovirus and coliphages in freshwater habitats is differentially affected by ambient sunlight and the presence of indigenous protozoa communities. Virol. J. 17, 1. [PubMed: 31906972]

Montoya D, 2015. Pollution in Sydney Harbour: sewage, toxic chemicals and microplastics. Briefing Paper No 03/2015.

Nelson KL, Boehm AB, Davies-Colley RJ, Dodd MC, Kohn T, Linden KG, Liu Y, Maraccini PA, McNeill K, Mitch WA, Nguyen TH, Parker KM, Rodriguez RA, Sassoubre LM, Silverman AI, Wigginton KR, Zepp RG, 2018. Sunlight-mediated inactivation of health-relevant microorganisms in water: a review of mechanisms and modeling approaches. Environ Sci Process Impacts 16, 1089–1122.

OEH, 2011. Beachwatch Programs. Protocol for Assessment and Management of Microbial Risks in Recreational Waters. Office of Environment and Heritage, NSW.

Ramírez-Castillo FY, Loera-Muro A, Jacques M, Garneau P, Avelar-González FJ, Harel J, Guerrero-Barrera AL, 2015. Waterborne pathogens: detection methods and challenges. Pathogens 4, 307–334. [PubMed: 26011827]

Rochelle-Newall E, Nguyen TM, Le TP, Sengtaheuanghoung O, Ribolzi O, 2015. A short review of fecal indicator bacteria in tropical aquatic ecosystems: knowledge gaps and future directions. Front. Microbiol. 6, 308. [PubMed: 25941519]

Rosario K, Symonds EM, Sinigalliano C, Stewart J, Breitbart M, 2009. Pepper mild mottle virus as an indicator of fecal pollution. Appl. Environ. Microbiol. 75, 7261–7267. [PubMed: 19767474]

Scott TM, Rose JB, Jenkins TM, Farrah SR, Lukasik J, 2002. Microbial source tracking: current methodology and future directions. Appl. Environ. Microbiol. 68, 5796–5803. [PubMed: 12450798]

Stachler E, Kelty C, Sivaganesan M, Li X, Bibby K, Shanks OC, 2017. Quantitative CrAssphage PCR assays for human fecal pollution measurement. Environ. Sci. Technol. 51, 9146–9154. [PubMed: 28700235]

Staley C, Gordon KV, Schoen ME, Harwood VJ, 2012. Performance of two quantitative PCR methods for microbial source tracking of human sewage and implications for microbial risk assessment in recreational waters. Appl. Environ. Microbiol. 78, 7317–7326. [PubMed: 22885746]

Steele JA, Blackwood AD, Griffith JF, Noble RT, Schiff KC, 2018. Quantification of pathogens and markers of fecal contamination during storm events along popular surfing beaches in San Diego, California. Water Res. 136, 137–149. [PubMed: 29501758]

Symonds EM, Verbyla EM, Lukasik JO, Kafle RC, Breitbart M, Mihelcic JR, 2014. A case study of enteric virus removal and insights into the associated risk of water reuse for two wastewater treatment pond systems in Bolivia. Water Res. 65, 257–270. [PubMed: 25129566]

Tiwari A, Oliver DM, Bivins A, Sherchan SP, Pitkänen T, 2021. Bathing water quality monitoring practices in Europe and the United States. Int. J. Environ. Res. Public Health 18, 5513. [PubMed: 34063910]

Tiwari A, Kauppinen A, Räsänen P, Salonen J, Wessels L, Juntunen J, Miettinen IT, Pitkänen T, 2023. Effects of temperature and light exposure on the decay characteristics of fecal indicators, norovirus, and Legionella in mesocosms simulating subarctic river water. Sci. Total Environ. 859 (Pt 2), 160340. [PubMed: 36423850]

Verbyla ME, Symonds EM, Kafle RC, Cairns MR, Iriarte M, Mercado Guzman A, Coronado O, Breitbart M, Ledo C, Mihelcic JR, 2016. Managing microbial risks from indirect wastewater reuse for irrigation in urbanizing watersheds. Environ. Sci. Technol. 50, 6803–6813. [PubMed: 26992352]

Wade TJ, Sams E, Brenner KP, Haugland R, Chern E, Beach M, Wymer L, Rankin CC, Love D, Li Q, Noble R, Dufour AP, 2010. Rapidly measured indicators of recreational water quality and

swimming-associated illness at marine beaches: a prospective cohort study. Environ. Health 9, 66. [PubMed: 21040526]

Whitman RL, Nevers MB, Korinek GC, Byappanahalli MN, 2004. Solar and temporal effects on Escherichia coli concentration at a Lake Michigan swimming beach. Appl. Environ. Microbiol. 70, 4276–4285. [PubMed: 15240311]

Wyn-Jones AP, Carducci A, Cook N, D'Agostino M, Divizia M, Fleischer J, Gantzer C, Gawler A, Girones R, Holler C, de Roda Husman AM, Kay D, Kozyra I, Lopez-Pila J, Muscillo M, Nascimento MSJ, Papageorgiou P, Rutjes S, Sellwood J, Szewzyk R, Wyer M, 2011. Surveillance of adenoviruses and noroviruses in European recreational waters. Water Res. 45, 1025–1038. [PubMed: 21093010]

HIGHLIGHTS

- HF183 decayed the fastest compared to PMMoV, which exhibited the slowest decay.
- Sunlight exposure significantly accelerated decay of HF183, Lachno3, and enterovirus.
- Enteric viruses showed faster decay than PMMoV and crAssphage.
- Decay rates vary between mesocosms, emphasizing the impact of sunlight exposure.

Table 1

Decay rates (*k*/day) and corresponding T_{90} values of human wastewater-associated marker and enteric viruses' nucleic acid in Davidson Park (DP) mesocosms.

Markers and enteric viruses	Treatments	Mean *k* (95 % CI slope)	R^2	RMSE	Runs test *p* value	Mean T_{90} days (95 % CI T_{90})
HF183	Sunlight	−0.414 (−0.457 to −0.370)	0.983	0.584	$p = 0.333$ (NS)	5.56 (5.03 to 5.48)
	Dark	−0.240 (−0.258 to −0.223)	0.990	0.432	$p = 0.900$ (NS)	9.59 (8.92 to 10.3)
Lachno3	Sunlight	−0.272 (−0.304. to −0.240)	0.969	0.644	$p = 0.500$ (NS)	8.46 (7.57 to 11.3)
	Dark	−0.182 (−0.194 to −0.170)	0.989	0.429	$p = 0.400$ (NS)	12.6 (11.9 to 13.5)
CrAssphage	Sunlight	−0.259 (−0.300 to −0.218)	0.945	0.832	$p = 0.500$ (NS)	8.88 (7.67 to 10.6)
	Dark	−0.233 (−0.267 to −0.198)	0.949	0.878	$p = 0.500$ (NS)	9.87 (8.62 to 11.6)
PMMoV	Sunlight	−0.162 (−0.192 to −0.133)	0.911	0.823	$p = 0.999$ (NS)	14.2 (12.0 to 17.3)
	Dark	−0.087 (−0.108 to −0.066)	0.795	1.036	$p = 0.300$ (NS)	26.5 (21.3 to 34.9)
HAdV 40/41	Sunlight	−0.237 (−0.362 to −0.106)	0.729	1.085	$p = 0.666$ (NS)	9.71 (6.35 to 21.7)
	Dark	−0.141 (−0.204 to −0.078)	0.688	0.773	$p = 0.500$ (NS)	16.3 (11.3 to 29.5)
EV	Sunlight	−0.268 (−0.524 to −0.011)	0.760	0.794	$p = 0.999$ (NS)	8.60 (4.39 to 209)
	Dark	−0.097 (−0.118 to −0.077)	0.937	0.350	$p = 0.500$ (NS)	23.7 (19.5 to 29.9)
HNoV GII	Sunlight	−0.181 (−0.266 to −0.096)	0.807	0.688	$p = 0.666$ (NS)	12.7 (8.65 to 24.0)
	Dark	−0.115 (−0.152 to −0.078)	0.917	0.301	$p = 0.666$ (NS)	24.0 (16.2 to 45.1)

NS: non-significant deviation from the model.

Table 2

Decay rates (*k*/day) and corresponding T_{90} values of human wastewater-associated marker and enteric viruses' nucleic acid in Hen and Chicken Bay mesocosms.

Markers and enteric viruses	Treatments	Mean *k* (95 % CI slope)	R^2	RMSE	Runs test *p* value	Mean T_{90} days (95 % CI T_{90})
HF183	Sunlight	−0.328 (−0.381 to −0.266)	0.937	1.169	$p = 0.900$ (NS)	7.01 (6.04 to 8.65)
	Dark	−0.195 (−0.221 to −0.170)	0.950	0.921	$p = 0.333$ (NS)	11.8 (10.4 to 13.5)
Lachno3	Sunlight	−0.201 (−0.222 to −0.180)	0.945	0.967	$p = 0.114$ (NS)	11.5 (10.4 to 12.8)
	Dark	−0.181 (−0.197 to −0.166)	0.962	0.727	$p = 0.114$ (NS)	12.7 (11.7 to 13.9)
CrAssphage	Sunlight	−0.289 (−0.351 to −0.226)	0.924	1.281	$p = 0.500$ (NS)	7.96 (6.55 to 10.2)
	Dark	−0.200 (−0.222 to −0.178)	0.953	0.784	$p = 0.200$ (NS)	11.5 (10.4 to 12.9)
PMMoV	Sunlight	−0.064 (−0.081 to −0.048)	0.805	0.749	$p = 0.371$ (NS)	36.0 (28.4 to 48.0)
	Dark	−0.056 (−0.079 to −0.034)	0.653	0.811	$p = 0.542$ (NS)	41.1 (29.1 to 67.1)
HAdV 40/41	Sunlight	−0.155 (−0.185 to −0.126)	0.946	0.396	$p = 0.999$ (NS)	14.9 (12.4 to 18.3)
	Dark	−0.129 (−0.144 to −0.113)	0.949	0.434	$p = 0.100$ (NS)	17.8 (17.8 to 20.4)
EV	Sunlight	−0.134 (−0.165 to −0.103)	0.921	0.417	$p = 0.333$ (NS)	18.9 (14.0 to 17.2)
	Dark	−0.113 (−0.156 to −0.071)	0.885	0.346	$p = 0.666$ (NS)	17.1 (14.7 to 32.4)
HNoV GII	Sunlight	−0.114 (−0.150 to −0.077)	0.862	0.490	$p = 0.666$ (NS)	20.2 (15.3 to 29.9)
	Dark	−0.147 (−0.186 to −0.097)	0.829	0.663	$p = 0.666$ (NS)	15.7 (12.4 to 23.7)

NS: non-significant deviation from the model.

Table 3

Comparison of decay rates (*k*/day) and corresponding T_{90} values of human wastewater-associated marker and enteric viruses' nucleic acid in Davidson Park (DP) and Hen and Chicken Bay (HCB) mesocosms with laboratory microcosms.

Markers and enteric viruses	Treatments	DP mesocosms (this study)		HCB mesocosms (this study)		Laboratory microcosms (Ahmed et al., 2023b)	
		Mean *k* (95 % CI slope)	Mean T_{90} days (95 % CI T_{90})	Mean *k* (95 % CI slope)	Mean T_{90} days (95 % CI T_{90})	Mean *k* (95 % CI slope)	Mean T_{90} days (95 % CI T_{90})
HF183	Sunlight	−0.414 (−0.457 to −0.370)	5.56 (5.03 to 5.48)	−0.328 (−0.381 to −0.266)	7.01 (6.04 to 8.65)	−0.481 (−0.611 to −0.351)	4.78 (3.76 to 6.56)
	Dark	−0.240 (−0.258 to −0.223)	9.59 (8.92 to 10.3)	−0.195 (−0.221 to −0.170)	11.8 (10.4 to 13.5)	−0.246 (−0.325 to −0.166)	9.36 (7.08 to 13.9)
Lachno3	Sunlight	−0.272 (−0.304. to −0.240)	8.46 (7.57 to 11.3)	−0.201 (−0.222 to −0.180)	11.5 (10.4 to 12.8)	−0.339 (−0.399 to −0.279)	6.79 (5.77 to 8.25)
	Dark	−0.182 (−0.194 to −0.170)	12.6 (11.9 to 13.5)	−0.181 (−0.197 to −0.166)	12.7 (11.7 to 13.9)	−0.100 (−0.118 to −0.082)	23.0 (19.5 to 28.1)
CrAssphage	Sunlight	−0.259 (−0.300 to −0.218)	8.88 (7.67 to 10.6)	−0.289 (−0.351 to −0.226)	7.96 (6.55 to 10.2)	−0.426 (−0.469 to −0.383)	5.40 (4.90 to 6.01)
	Dark	−0.233 (−0.267 to −0.198)	9.87 (8.62 to 11.6)	−0.200 (−0.222 to −0.178)	11.5 (10.4 to 12.9)	−0.110 (−0.128 to −0.091)	20.9 (18.0 to 25.3)
PMMoV	Sunlight	−0.162 (−0.192 to −0.133)	14.2 (12.0 to 17.3)	−0.064 (−0.081 to −0.048)	36.0 (28.4 to 48.0)	−0.044 (−0.058 to −0.029)	52.3 (39.7 to 79.4)
	Dark	−0.087 (−0.108 to −0.066)	26.5 (21.3 to 34.9)	−0.056 (−0.079 to −0.034)	41.1 (29.1 to 67.1)	−0.060 (−0.076 to −0.044)	38.4 (30.3 to 52.3)
HAdV 40/41	Sunlight	−0.237 (−0.362 to −0.106)	9.71 (6.35 to 21.7)	−0.155 (−0.185 to −0.126)	14.9 (12.4 to 18.3)	−0.280 (−0.313 to −0.247)	8.22 (7.35 to 9.32)
	Dark	−0.141 (−0.204 to −0.078)	16.3 (11.3 to 29.5)	−0.129 (−0.144 to −0.113)	17.8 (17.8 to 20.4)	−0.089 (−0.107 to −0.071)	25.9 (21.5 to 32.4)
EV	Sunlight	−0.268 (−0.524 to −0.011)	8.60 (4.39 to 209)	−0.134 (−0.165 to −0.103)	18.9 (14.0 to 17.2)	−0.450 (−0.585 to −0.315)	5.11 (3.93 to 7.30)
	Dark	−0.097 (−0.118 to −0.077)	23.7 (19.5 to 29.9)	−0.113 (−0.156 to −0.071)	17.1 (14.7 to 32.4)	−0.248 (−0.366 to −0.129)	9.28 (6.29 to 17.8)
HNoV GII	Sunlight	−0.181 (−0.266 to −0.096)	12.7 (8.65 to 24.0)	−0.114 (−0.150 to −0.077)	20.2 (15.3 to 29.9)	N/A	N/A
	Dark	−0.115 (−0.152 to −0.078)	24.0 (16.2 to 45.1)	−0.147 (−0.186 to −0.097)	15.7 (12.4 to 23.7)	N/A	N/A

N/A: not applicable.